Vibronic coupling to simulate the phosphorescence spectra of Ir(III)-based OLED systems: TD-DFT results meet experimental data

H. Belaidi, S. Belaidi, Claudine Katan, C. Latouche, A. Boucekkine

▶ **To cite this version:**

H. Belaidi, S. Belaidi, Claudine Katan, C. Latouche, A. Boucekkine. Vibronic coupling to simulate the phosphorescence spectra of Ir(III)-based OLED systems: TD-DFT results meet experimental data. Journal of Molecular Modeling, 2016, 22 (11), pp.265. 10.1007/s00894-016-3132-8 . hal-01398045

HAL Id: hal-01398045

https://univ-rennes.hal.science/hal-01398045v1

Submitted on 14 Dec 2016

HAL is a multi-disciplinary open access archive for the deposit and dissemination of scientific research documents, whether they are published or not. The documents may come from teaching and research institutions in France or abroad, or from public or private research centers.

L'archive ouverte pluridisciplinaire **HAL**, est destinée au dépôt et à la diffusion de documents scientifiques de niveau recherche, publiés ou non, émanant des établissements d'enseignement et de recherche français ou étrangers, des laboratoires publics ou privés.

Vibronic Coupling to Simulate the Phosphorescence Spectra of Ir(III) Based OLED Systems: TD-DFT Results Meet Experimental Data

Houmam Belaidi[a,b], Salah Belaidi[b], Claudine Katan[a], Camille Latouche[c*], Abdou Boucekkine[a*]

[a] Institut des Sciences Chimiques de Rennes, UMR 6226 CNRS-Université de Rennes 1, Campus de Beaulieu, 35042 Rennes cedex, France
[b] département de chimie, Université Mohamed Khider, 07000 Biskra, Algeria
[c] Institut des Matériaux Jean Rouxel (IMN), Université de Nantes, CNRS, 2 rue de la Houssinière, BP 32229, 44322 Nantes Cedex 03, France

E-mail : abdou.boucekkine@univ-rennes1.fr; camille.latouche@cnrs-imn.fr

Abstract

In this paper we investigate theoretically the electronic and optical properties of six based Iridium imidazolylidene complexes (numbered **1a**, **1b**, **2, 2b, 3, 3b**) serving as serious candidates for OLED systems. Computations using methods rooted into DFT and TD-DFT explain the observed optical properties. Observed absorption bands have been assigned and computations of the lowest triplet excited states have been performed. Whereas complexes **1a** and **1b** are non-emissive in solution, the simulated phosphorescence spectra of complexes **2, 2b 3, 3b** taking into account the vibrational contributions to the electronic transitions fit nicely the observed ones. The use of vibronic coupling permitted to reproduce and explain the structured phosphorescence spectrum of complexes **2** and **2b**, as well as the absence of such structure for complexes **3** and **3b**.

Keywords: Iridium complexes; phosphorescence; TD-DFT; vibronic coupling; VMS software.

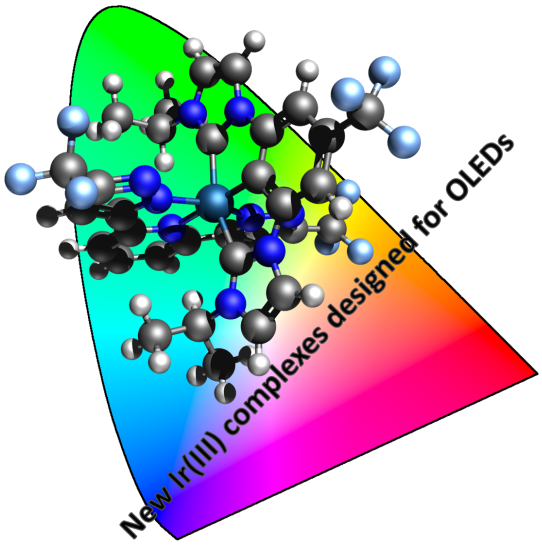

Introduction

In the past decades, transition metal complexes have been extensively studied, especially thanks to their strong ability to luminesce. Furthermore, compounds demonstrating a high emission response to stimuli are of interest for the development of organic light-emitting diodes (OLED) systems or light-emitting cells (LEC).[1–3] Among them, iridium complexes possess strong ability to emit light in a large energetic range.[4–10] Furthermore, iridium, ruthenium or platinum complexes are among the most investigated compounds and numerous studies from both the experimental and computational sides have been reported due to their strong ability to be embedded in devices.[4, 5, 8–17]

From an experimental point view, it remains challenging and difficult to fully characterize the electronic processes at work within the targeted compounds. As a matter of fact, chemists performing quantum chemical computations are now able to give crucial information on these electronic processes, namely those relevant to excitation and emission phenomena and the nature of the reached excited states, especially thanks to the very recent developments in this area.[18–23] Moreover, Density Functional Theory (DFT) and its time dependent extension (TD-DFT) are now routinely used to get both electronic and vibrational information from small organic to large-size organometallic and transition metal complexes systems.[10,24–30] Indeed, DFT calculations are now accurate enough to predict or confirm the stability or existence of compounds, and they can also explain the luminescent and/or spectroscopic properties of complex systems. [31–40]

In the field of spectroscopy calculations, Vlcek Jr. and Zális among other authors, have shown how DFT and TD-DFT are useful tools to study d^6 metal complexes.[41]

The computation of the vibrational structure of electronic absorption or emission bands should permit to reproduce more accurately both the position and the band shape of the observed spectra. In this context, Barone and coworkers implemented recently the so called Virtual Multifrequency Spectrometer (VMS)[42, 43] which is a powerful, mature and cheap tool to simulate accurately many types of spectra, even when one aims to investigate large systems or a large number of effects (solvent, anharmonicity and Duschinsky couplings).[50–59] Indeed, in the last years, the VMS approach has been used to simulate with high precision anharmonic and phosphorescence spectra of organometallics and transition metal complexes. [9, 18, 21–23]

New tridentate chelate Ir(III) complexes have been very recently synthesized and characterized by Chi and co-workers [personal communication]. These neutral complexes (Scheme 1) involving *bis*(imidazolylidene) benzene and 2-(5-trifluoromethyl-1H-pyrazol-3-yl)-6-(2,4-difluorophenyl) pyridine ($pzpyF_2p$) or 2,6-bis(5-trifluoromethylpyrazol-3-yl) pyridine (pz_2py) ligands, exhibit phosphorescence at short wavelengths very suitable for OLED devices. Interestingly, it is observed that complex **1** does not phosphor in solution, contrarily to complexes **2** and **3**, but all complexes emit when suitably processed as films. Moreover, whereas complexes **2** and **2b** exhibit a structured emission band, it is not the case for complexes **3** and **3b** that exhibit a structureless phosphorescence band.

In this paper, we report a full quantum investigation based on DFT and TD-DFT methods of these Ir(III) complexes in order to explain the observed properties and to provide guidance for the design of complexes of technological interest. We first discuss the ground state (GS) characteristics, *i.e.* the geometric and electronic structures. In a second step we focus our attention on the optical properties. We propose an assignment of the observed absorption band using TD-DFT. Then, the lowest triplet excited state (ES) will be studied. The combinations of these computations together with the aforementioned powerful tools, namely taking into account vibronic couplings, allows us to rationalize the observed properties.

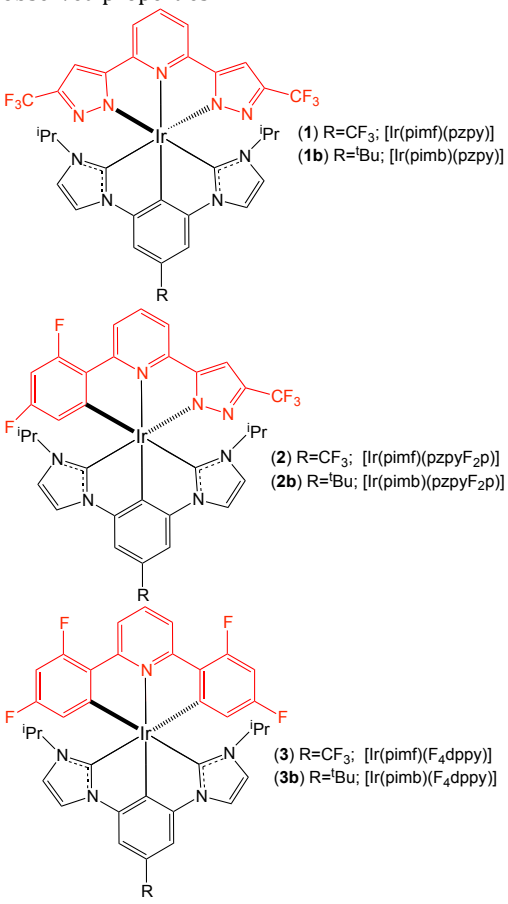

Scheme 1. Investigated bis-tridentate Ir(III) complexes.

Computational details

All calculations have been performed at the DFT level of theory employing the G09 suite of programs.[59] On the basis of several previous studies,[9, 10, 22] we have chosen the B3PW91 functional to perform the computations.[60–62] The associated basis set is the so-called LANL2DZ one, including a pseudopotential for

inner electrons of Ir and augmented with polarization functions on C(d; exponent 0.587), N(d; 0.736), F(d; 1.577) Ir(f; 0.938).[63–66] Solvent effects (CH_2Cl_2) have been taken into account by the Polarizable Continuum Model (PCM).[67, 68] All the GS geometries have been optimized and checked to be true minima on the Potential Energy Surface (PES), *i.e.* the computed frequencies of their normal modes of vibration are all real. Grimme's corrections for dispersion with Becke-Johnson damping (GD3BJ) have also been included in the computations.[69] Time-Dependent Density Functional Theory (TD-DFT) computations have been performed, using the optimized ground state geometries, to obtain excitations energies and spectra. Then, in order to plot the phosphorescence spectra, vibronic contributions to electronic emission have been considered using the Adiabatic Shift (AS) approach as implemented in the used version of the Gaussian Package.[42,70] The optimized geometries and vibration frequencies of the first triplet state have been obtained using unrestricted calculations. Spin-orbit coupling and Herzberg-Teller terms have not been taken into account in the calculations. Orbital visualization has been done using the GaussView[71] program and the orbital composition has been obtained using the AOmix package.[72] The simulated UV-visible and phosphorescence spectra have been respectively plotted using the Swizard[73] and the VMS programs.[43]

Results and discussion

Ground state geometric structures

The optimized geometries are compared with the experimental data (Table 1 and ESI). In this section the discussion of the geometry will focuse on complex **1** but trends are similar for the other compounds.

Table 1. Selected experimental and computed structural data of complex **1**.

Bond lengths (Å)	**Ir-C**	**Ir-N**	
X-ray	1.965(5) 2.078(5) 2.056(4)	2.046(3) 2.052(4) 2.038(4)	
DFT	1.969 2.039 2.040	2.028 2.047 2.031	
Angles (°)	**C-Ir-C**	**N-Ir-N**	**C-Ir-N**
X-ray	154.9(18)	155.6(15)	178.7(18)
DFT	155.7	156.9	179.5

In average the computed M-L bond lengths fit nicely the observed ones, even if a slight underestimation in the simulation is observed. The angles around the metal are also well reproduced in our calculations with a deviation of less than 1° in comparison to the X-ray data. This trend also matches what some of us have reported before, *i. e.* the methodology (B3PW91/LANL2DZ+pol.) provides very accurate geometries in the simulations with respect to X-ray experiments.[9, 10]

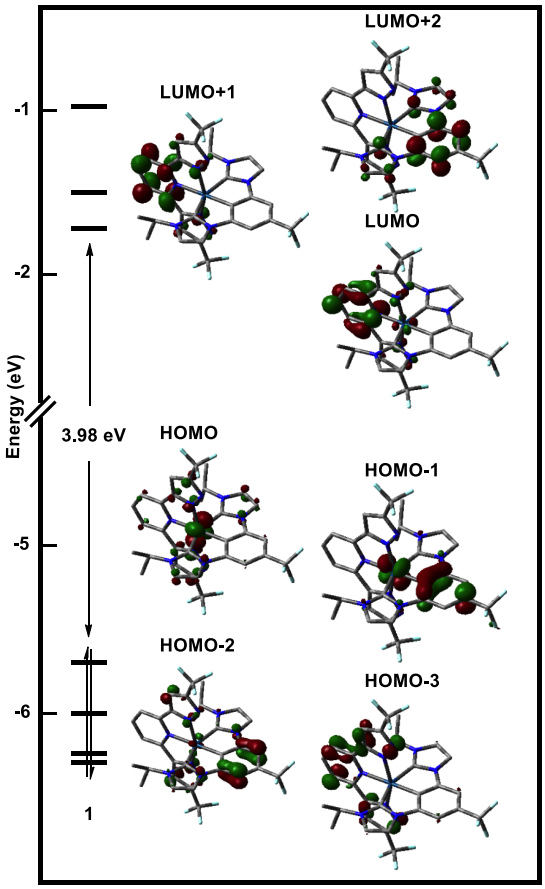

Figure 1. Frontier orbitals diagram of complex **1**.

Ground state electronic structures and electronic vertical excitations

We now focus our attention on the electronic structures. On the optimized GS geometries, TD-DFT vertical excitations computations have been performed. The charge transfers occurring during excitations for the six complexes are described thanks to their electronic structures. As the *pimf* and *pimb* ligands (scheme 1) differ only by replacing a CF_3 by a ^{t}Bu group on the benzene ring, the properties of their related complexes (*e.g.* **1**, **1b**) are relatively similar; therefore the discussion will mainly focuse on complexes **1**, **2** and **3**. Furthermore, as we found that the frontier orbitals are similar for all complexes, only the molecular orbital (MO) diagram of **1** is discussed (Figure 1; MO diagrams for **1b**, **2b** and **3b** are in ESI)). The highest occupied molecular orbitals (HOMO) are mainly localized on the metal atom (*d* orbitals) whereas the lowest unoccupied orbitals (LUMO) are π^* types localized on the ligands.. One should mention that, as expected, the CF_3 moieties are not involved in the frontier orbitals.

Using the GS optimized geometries, TD-DFT calculations have been performed to simulate the electronic absorption spectra based on the vertical excitations, and compared to the experimental ones (Figure 2).

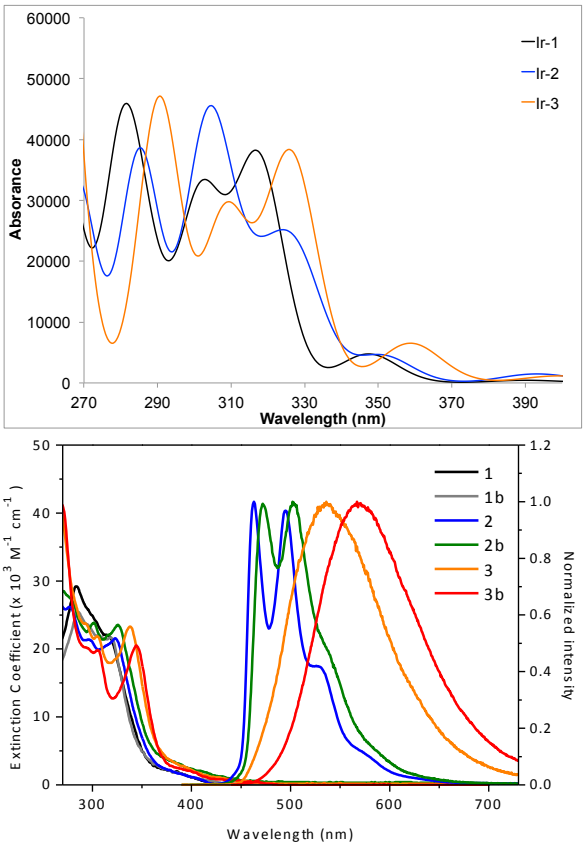

Figure 2. Simulated absorption (top) and Observed Absorption and Luminescence Spectra (bottom).

The experimental and simulated absorption spectra are in good agreement; both the computed transition energies and intensities fit nicely the experimental data. Furthermore, the observed absorption red shift between complexes **1** and **3** is also well reproduced in the simulations. It turns out that the modulation of the ligand also tunes the absorption bands. Indeed, a small red shift occurs when *pimb* ligand is used instead of *pimf*. This trend is also well portrayed in the simulations.

In order to assign the transition bands, the MOs compositions are collected in Table S1. and the experimental and calculated electronic transitions are provided in Table 2 and Table 3. All complexes exhibit a very weak absorption band around 400 nm and an intense one between 315 and 345 nm. As it can be seen in scheme 1, complex **2** derives from complex **1** replacing one pyrazolyl ring by a difluorophenyl one, and complex **3** is obtained by substituting the remaining pyrazolyl ring of complex **2** by a second difluorophenyl one. The latter ring being more conjugated, one expects that its contribution to the frontier MOs will be higher than the pyrazolyl ring one, leading to smaller energy gaps between occupied and vacant MOs, thus likely to explain partly the observed red shifts. Indeed, for complex **2** the difluorophenyl contribution appears in HOMO, HOMO-3, LUMO and LUMO+2 whereas the pyrazolyl is involved mainly in LUMO+1 HOMO-2 and HOMO-3. For complex **3** that bears two difluorophenyl, this effect is more important, namely their contribution to the frontier MOs, thus explaining the higher red shift observed for this complex.

Table 2. Experimental and calculated vertical excitations maxima.

Cplx	λ_{Exp} /nm (ε)[a]	λ_{Calc}/nm (f)[b]	λ_{max}/nm
1	316 (21.9) 406 (0.8)	317 (0.204) 320 0.033) 390 (0.003)	317 390
1b	318 (21.7) 409 (0.9)	309 (0.146) 322(0.204) 397 (0.002)	318 397
2	323 (21.6) 407 (0.9)	318 (0.079) 328 (0.130) 393 (0.010)	324 393
2b	325 (23.5) 418 (1.7)	324 (0.072) 334 (0.111) 401 (0,007)	329 400
3	338 (23.3) 431 (0.9)	325 (0.070) 327 (0.183) 399 (0.008)	326 399
3b	345 (20.4) 433 (0.7)	332 (0.309) 333 (0.156) 407(0.005)	333 407

[a] 10^{-3} M^{-1} cm^{-1}

[b] Oscillator strengths

Table 3. Band assignments of complexes **1** and **2**.

λ_{Calc} (nm)	f	Transitions
	1	
390	0.003	HOMO ⟶ LUMO (98%)
347	0.033	HOMO ⟶ LUMO+1 (89%)
320	0.033	HOMO-3 ⟶ LUMO (52%) HOMO-2 ⟶ LUMO+1 (39%)
317	0.204	HOMO-2 ⟶ LUMO (72%)
302	0.209	HOMO-2 ⟶ LUMO+1 (54%) HOMO-3 ⟶ LUMO (42%)
280	0.239	HOMO-3 ⟶ LUMO+1 (82%)
	2	
393	0.010	HOMO → LUMO (95%)
351	0.031	HOMO → LUMO+1 (86%) HOMO-2 → LUMO (10%)
328	0.130	HOMO-2 → LUMO (74%)
318	0.079	HOMO-3 → LUMO (50%) HOMO-2 → LUMO+1 (31%)
305	0.230	HOMO-2 → LUMO+1 (56%) HOMO-3 → LUMO (36%)
285	0.217	HOMO-1 → LUMO+3 (44%) HOMO-3 → LUMO+1 (27%)

From Table 3, it is clear that for complexes **1** and **2** the lowest energy excitations correspond to HOMO → LUMO transitions. It corresponds to a Metal to Ligand Charge Transfer (MLCT). A similar trend is observed for other excitations despite that the HOMO-3, which is localized on the π orbitals of the pyridine ligand, becomes involved for transitions at higher energy. Indeed, it turns out that the highest energy excitations reported for complex **1** is mainly a HOMO-3 to LUMO+1 (82%) transition, whereas for complex **2** it is an admixture of two excitations with a weak involvement of this particular transition (27 %).

Luminescence properties

Experimentally, contrarily to complexes **2** and **3**, complex **1** did not exhibit any luminescence signature in solution, but only when processed as a film [to be published]. Complexes **2** and **3** exhibit interesting and different luminescence properties (Figure 2). Indeed complex **2** shows a structured emission band whereas complex **3** possesses a single band. Such difference is a good challenge for state-of-the-art simulations tools. For instance, the reliability of the VMS on phosphorescence spectra, especially on transition metal complexes, has seldom been investigated.[9, 10, 22] First, we compute the excited state (ES) geometry. As one can see in Figure 3, the GS and ES geometries of complex **2** are almost identical. On the contrary, the ES and GS geometries of complex **3** show sizeable differences, but they remain similar enough to reasonably allow the vibronic treatment to be performed on these grounds.

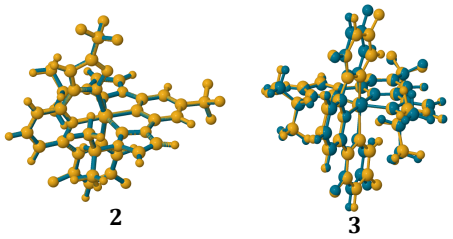

Figure 3. Superimposed GS and ES geometries of complexes **2** (left) and **3** (right).

Experimental spectra shown Figure 2, reveal that complexes **3** and **3b** have their absorption and emission maxima redshifted with respect to complexes **2** and **2b**. Furthermore, complexes with *pimb* ligand (**2b** and **3b**) also exhibit a redshift in comparison to complexes with *pimf* ligand (**2** and **3**). Figure 4 shows that these trends are nicely reproduced in our simulated spectra. The band maxima of experiment and simulations are also in a good agreement despite a small underestimation (less than 50 nm) of the maxima. Concerning the band shapes, the agreement is noteworthy. In fact, if one inspects the spectra of complexes **2** and **2b**, three maxima, one shoulder and a long tail are observed. This band structure is perfectly reproduced in our simulations. It turns out that the relative intensities are also well described in the simulations but the absolute intensities remain underestimated, especially for the second maxima. Finally, a small red shift is also observed between the absorption bands of complexes **1**, **2**, **3** and **1b**, **2b**, **3b**, respectively, reminding that the difference between their structures is the substitution of the electron withdrawing CF_3 group by the ^{t}Bu donating one. Whereas the CF_3 group induces a lowering of the LUMO, the ^{t}Bu leads to an increase of the HOMO energies, so that their effects are in the same direction regarding the reduction of the HOMO-LUMO energy gap. However, replacing one group by the other one leads to cancel the lowering effect induced by the first one. Considering the observed red shifts, it can be concluded that the effect of the donating group is slightly more important to reduce this gap than the effect of the electron withdrawing group. Indeed, in our case, the HOMO-LUMO gap is reduced by 0.1-0.2 eV when replacing CF_3 by ^{t}Bu.

Finally, complexes **3** and **3b** exhibit a structureless emission band centred around 550 nm. This sharp band is also nicely reproduced in the simulation. The emission spectra of complexes **2** and **2b** exhibit several bands contrarily to complexes **3** and **3b**. Vibration modes of the *pzpyF2p* ligand, which is involved in the lowest virtual MOs, appear to participate to the vibronic structure of the emission spectrum of complex **2** computed using the adiabatic shift approach (see computational details); these facts are likely to explain the structured phosphorescence spectrum of this complex. On the contrary, such an influence of ligand on the emission spectrum is not observed for complex **3**. One of the tools to characterize the principal vibrational progressions and the normal modes involved in the electronic transition in the AS method that we used, is called the shift vector (Figures S7 and S8 for complexes 2 and 3, respectively). The shift vector corresponds to the gradient of the final state projected on the normal modes of the initial state.[22] The shift vectors of complexes 2 and 3 are rather different. Indeed, it appears that complex 2 possesses more normal modes with a strong shift vector (Figure S7) than complex 3 (Figure S8), leading to a larger vibrational contribution to the electronic transition. This fact could explain the differences in the phosphorescence spectra between both complexes.

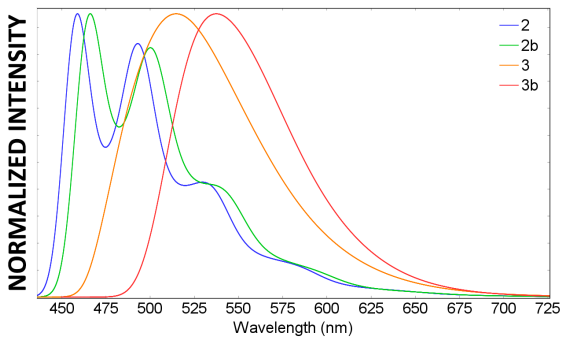

Figure 4. Simulated Phosphorescence Spectra of Complexes **2**, **2b**, **3** and **3b**.

Conclusion

In this article we have provided explanations of the optical (absorption and emission) properties of six new iridium complexes using quantum chemistry computations. As recently stated by some authors, the computational protocol that we used to perform excited state investigations on Ir(III) complexes seems to be efficient, *e. g.* B3PW91/LANL2DZ+pol.[9, 10] Complexes **2** and **3** have shown a strong phosphorescence signature, which have been nicely reproduced and rationalized in our simulations. Indeed, the simulated phosphorescence spectra using the VMS approach allowed a direct vis-à-vis between experiment and simulations.

Acknowledgements

Prof. Yun Chi (National Tsing Hua University, Taiwan), who communicated his experimental results prior to publication, and Prof. Vincenzo Barone (SNS Pisa, Italy), who made available the VMS package developed in his laboratory, are gratefully acknowledged. We also acknowledge the HPC resources of CINES and of IDRIS under the allocations 2015-[x2015080649] and 2016-[x2016080649] made by GENCI (Grand Equipement National de Calcul Intensif).

Electronic Supplementary Information

Ground state optimized geometries of all complexes. Orbital diagrams of complexes **1b**, **2**, **2b**, **3**, **3b**. Simulated electronic absorption spectra of complexes **1b**, **2b** and **3b**. Shift vectors/normal modes of complexes **2** and **3**. Energies and 5d metal orbital weights of frontier MOs of complexes **1a**, **1b – 3a**, **3b**.

References

1. D'Andrade BW, Forrest SR (2004) White Organic Light-Emitting Devices for Solid-State Lighting. Adv Mater 16:1585–1595. doi: 10.1002/adma.200400684
2. Sun Y, Forrest SR (2007) High-efficiency white organic light emitting devices with three separate phosphorescent emission layers. Appl Phys Lett 91:263503. doi: http://dx.doi.org/10.1063/1.2827178
3. Chen C-Y, Pootrakulchote N, Chen M-Y, et al (2012) A New Heteroleptic Ruthenium Sensitizer for Transparent Dye-Sensitized Solar Cells. Adv Energy Mater 2:1503–1509. doi: 10.1002/aenm.201200285
4. Schulze M, Steffen A, Würthner F (2015) Near-IR Phosphorescent Ruthenium(II) and Iridium(III) Perylene Bisimide Metal Complexes. Angew Chemie Int Ed 54:1570–1573. doi: 10.1002/anie.201410437
5. Angelis F De, Belpassi L, Fantacci S (2009) Spectroscopic properties of cyclometallated iridium complexes by TDDFT. J Mol Struct THEOCHEM 914:74–86. doi: http://dx.doi.org/10.1016/j.theochem.2009.07.025
6. Dragonetti C, Colombo A, Marinotto D, et al (2014) Functionalized styryl iridium (III) complexes as active second-order NLO chromophores and building blocks for SHG polymeric films. J Organomet Chem 751:568–572.
7. Broeckx LEE, Delaunay W, Latouche C, et al (2013) C-H activation of 2,4,6-triphenylphosphinine: synthesis and characterization of the first homoleptic phosphinine-iridium(III) complex fac-[Ir(C^P)3]. Inorg Chem 52:10738–40. doi: 10.1021/ic401933m
8. Sun H, Liu S, Lin W, et al (2014) Smart responsive phosphorescent materials for data recording and security protection. Nat Commun 5:3601. doi: 10.1038/ncomms4601
9. Vazart F, Latouche C (2015) Validation of a computational protocol to simulate near IR phosphorescence spectra for Ru(II) and Ir(III) metal complexes. Theor Chem Acc 134:1–7. doi: 10.1007/s00214-015-1737-0
10. Latouche C, Skouteris D, Palazzetti F, Barone V (2015) TD-DFT Benchmark on Inorganic Pt(II) and Ir(III) Complexes. J Chem Theory Comput 11:3281–3289. doi: 10.1021/acs.jctc.5b00257
11. Heinze K, Hempel K, Tschierlei S, et al (2009) Resonance Raman Studies of Bis(terpyridine)ruthenium(II) Amino Acid Esters and Diesters. Eur J Inorg Chem 2009:3119–3126. doi: 10.1002/ejic.200900309
12. Bhuiyan A a., Kincaid JR (1998) Synthesis and Photophysical Properties of Zeolite-Entrapped Bisterpyridine Ruthenium(II). Dramatic Consequences of Ligand-Field-State Destabilization. Inorg Chem 37:2525–2530. doi: 10.1021/ic970950u
13. Muhavini Wawire C, Jouvenot D, Loiseau F, et al (2013) Density-functional study of luminescence in polypyridine ruthenium complexes. J Photochem Photobiol A Chem 276:8–15. doi: http://dx.doi.org/10.1016/j.jphotochem.2013.10.018
14. Bergeron B V, Meyer GJ (2002) Reductive Electron Transfer Quenching of MLCT Excited States Bound To Nanostructured Metal Oxide Thin Films. J Phys Chem B 107:245–254. doi: 10.1021/jp026823n
15. Johansson PG, Kopecky A, Galoppini E, Meyer GJ (2013) Distance Dependent Electron Transfer at TiO2 Interfaces Sensitized with Phenylene Ethynylene Bridged RuII–Isothiocyanate Compounds. J Am Chem Soc 135:8331–8341. doi: 10.1021/ja402193f
16. Lundqvist MJ, Galoppini E, Meyer GJ, Persson P (2007) Calculated Optoelectronic Properties of Ruthenium Tris-bipyridine Dyes Containing Oligophenyleneethynylene Rigid Rod Linkers in Different Chemical Environments. J Phys Chem A 111:1487–1497. doi: 10.1021/jp064219x
17. Schoonover JR, Bates WD, Meyer TJ (1995) Application of Resonance Raman Spectroscopy to Electronic Structure in Metal Complex Excited States. Excited-State Ordering and Electron Delocalization in Dipyrido[3,2-a:2',3'-c]phenazine (dppz): Complexes of

Re(I) and Ru(II). Inorg Chem 34:6421–6422. doi: 10.1021/ic00130a004
18. Latouche C, Baiardi A, Barone V (2014) Virtual Eyes Designed for Quantitative Spectroscopy of Inorganic Complexes: Vibronic Signatures in the Phosphorescence Spectra of Terpyridine Derivatives. J. Phys. Chem. B 119:7253-7257. doi: 10.1021/jp510589u
19. Barone V, Biczysko M, Bloino J (2014) Fully anharmonic IR and Raman spectra of medium-size molecular systems: accuracy and interpretation. Phys Chem Chem Phys 16:1759–1787. doi: 10.1039/C3CP53413H
20. Biczysko M, Panek P, Scalmani G, et al (2010) Harmonic and Anharmonic Vibrational Frequency Calculations with the Double-Hybrid B2PLYP Method : J Chem Theory Comput 6:2115–2125.
21. Baiardi A, Bloino J, Barone V (2015) "Accurate simulation of Resonance-Raman spectra of flexible molecules: an internal coordinates approach." J Chem Theory Comput DOI:10.1021/acs.jctc.5b00241. doi: 10.1021/acs.jctc.5b00241
22. Vazart F, Latouche C, Bloino J, Barone V (2015) Vibronic Coupling Investigation to Compute Phosphorescence Spectra of Pt(II) Complexes. Inorg Chem 54:5588–5595. doi: 10.1021/acs.inorgchem.5b00734
23. Latouche C, Palazzetti F, Skouteris D, Barone V (2014) High-Accuracy Vibrational Computations for Transition Metal Complexes Including Anharmonic Corrections: Ferrocene, Ruthenocene and Osmocene as test cases. J Chem Theory Comput 10:4565–4573. doi: 10.1021/ct5006246
24. Green K, Gauthier N, Sahnoune H, et al (2013) Covalent Immobilization of Redox-Active Fe(κ2-dppe)(η5-C5Me5)-Based π-Conjugated Wires on Oxide-Free Hydrogen-Terminated Silicon Surfaces. Organometallics 32:5333–5342. doi: 10.1021/om4006017
25. Sahnoune H, Baranová Z, Bhuvanesh N, et al (2013) A Metal-Capped Conjugated Polyyne Threaded through a Phenanthroline-Based Macrocycle. Probing beyond the Mechanical Bond to Interactions in Interlocked Molecular Architectures. Organometallics 32:6360–6367. doi: 10.1021/om400709q
26. Makhoul R, Sahnoune H, Davin T, et al (2014) Proton-Controlled Regioselective Synthesis of [Cp*(dppe)Fe–C≡C-1-(η 6 -C 10 H 7)Ru(η 5 -Cp](PF 6) and Electron-Driven Haptotropic Rearrangement of the (η 5 -Cp)Ru + Arenophile. Organometallics 33:4792–4802. doi: 10.1021/om500047k
27. Green K, Gauthier N, Sahnoune H, et al (2013) Synthesis and Characterization of Redox-Active Mononuclear Fe(κ2-dppe)(η5-C5Me5)-Terminated π-Conjugated Wires. Organometallics 32:4366–4381. doi: 10.1021/om400515g
28. Latouche C, Liu CW, Saillard J-Y (2014) Encapsulating Hydrides and Main-Group Anions in d10-Metal Clusters Stabilized by 1,1-Dichalcogeno Ligands. J Clust Sci 25:147–171. doi: 10.1007/s10876-013-0671-3
29. Liao J-H, Latouche C, Li B, et al (2014) A twelve-coordinated iodide in a cuboctahedral silver(I) skeleton. Inorg Chem 53:2260–7. doi: 10.1021/ic402960e
30. Latouche C, Lin Y-R, Tobon Y, et al (2014) Au-Au chemical bonding induced by UV irradiation of dinuclear gold(I) complexes: a computational study with experimental evidence. Phys Chem Chem Phys 16:25840–5.
31. Boixel J, Guerchais V, Le Bozec H, et al (2014) Second-Order NLO Switches from Molecules to Polymer Films Based on Photochromic Cyclometalated Platinum(II) Complexes. J Am Chem Soc 136:5367–5375. doi: 10.1021/ja4131615
32. Jacquemin D, Perpète EA, Scuseria GE, et al (2008) TD-DFT Performance for the Visible Absorption Spectra of Organic Dyes: Conventional versus Long-Range Hybrids. J Chem Theory Comput 4:123–135. doi: 10.1021/ct700187z
33. Steffen A, Costuas K, Boucekkine A, et al (2014) Fluorescence in Rhoda- and Iridacyclopentadienes Neglecting the Spin–Orbit Coupling of the Heavy Atom: The Ligand Dominates. Inorg Chem 53:7055–7069. doi: 10.1021/ic501115k
34. Jacquemin D, Perpète EA, Scuseria GE, et al (2008) Extensive TD-DFT investigation of the first electronic transition in substituted azobenzenes. Chem Phys Lett 465:226–229. doi: http://dx.doi.org/10.1016/j.cplett.2008.09.071
35. Jacquemin D, Preat J, Wathelet V, et al (2006) Thioindigo Dyes: Highly Accurate Visible Spectra with TD-DFT. J Am Chem Soc 128:2072–2083. doi: 10.1021/ja056676h
36. Latouche C, Barone V (2014) Computational Chemistry Meets Experiments for Explaining the Behavior of Bibenzyl: A Thermochemical and Spectroscopic (Infrared, Raman, and NMR) Investigation. J Chem Theory Comput 10:5586–5592. doi: 10.1021/ct500930b
37. Latouche C, Kahlal S, Furet E, et al (2013) Shape Modulation of Octanuclear Cu (I) or Ag (I) Dichalcogeno Template Clusters with Respect to the Nature of their Encapsulated Anions: A Combined Theoretical and Experimental Investigation. Inorg Chem 52:7752–7765.
38. Latouche C, Kahlal S, Lin Y-R, et al (2013) Anion Encapsulation and Geometric Changes in Hepta-and Hexanuclear Copper (I) Dichalcogeno Clusters: A Theoretical and Experimental Investigation. Inorg Chem 52:13253–13262.
39. Latouche C, Lanoe P-H, Williams JAG, et al (2011) Switching of excited states in cyclometalated platinum complexes incorporating pyridyl-acetylide ligands (Pt--C [triple bond, length as m-dash] C--py): a combined experimental and theoretical study. New J Chem 35:2196–2202.
40. Barone V, Latouche C, Skouteris D, et al (2015) Gas-phase formation of the prebiotic molecule formamide: insights from new quantum computations. Mon Not R Astron Soc Lett 453:L31–L35.
41. Vlček A, Záliš S (2007) Modeling of charge-transfer transitions and excited states in d6 transition

metal complexes by DFT techniques. Coord Chem Rev 251:258–287. doi: 10.1016/j.ccr.2006.05.021
42. Barone V, Baiardi A, Biczysko M, et al (2012) Implementation and validation of a multi-purpose virtual spectrometer for large systems in complex environments. Phys Chem Chem Phys 14:12404–12422. doi: 10.1039/C2CP41006K
43. Licari D, Baiardi A, Biczysko M, et al (2015) Implementation of a graphical user interface for the virtual multifrequency spectrometer: The VMS-Draw tool. J Comput Chem 36:321–334.
44. Barone V (2016) The virtual multifrequency spectrometer: a new paradigm for spectroscopy. Wiley Interdiscip Rev Comput Mol Sci 6:86–110. doi: 10.1002/wcms.1238
45. Bloino J, Barone V (2012) A second-order perturbation theory route to vibrational averages and transition properties of molecules: General formulation and application to infrared and vibrational circular dichroism spectroscopies. J Chem Phys 136:124108. doi: http://dx.doi.org/10.1063/1.3695210
46. Barone V (2012) Computational Strategies for Spectroscopy. John Wiley {{}{&}{}} Sons Inc., Hoboken, New Jersey
47. Barone V, Biczysko M, Bloino J, et al (2012) Toward anharmonic computations of vibrational spectra for large molecular systems. Int J Quantum Chem 112:2185–2200. doi: 10.1002/qua.23224
48. Piccardo M, Bloino J, Barone V (2015) Generalized vibrational perturbation theory for rotovibrational energies of linear, symmetric and asymmetric tops: Theory, approximations, and automated approaches to deal with medium-to-large molecular systems. Int J Quantum Chem 115:948–982. doi: 10.1002/qua.24931
49. Egidi F, Bloino J, Barone V, Cappelli C (2012) Toward an Accurate Modeling of Optical Rotation for Solvated Systems: Anharmonic Vibrational Contributions Coupled to the Polarizable Continuum Model. J Chem Theory Comput 8:585–597.
50. Baiardi A, Bloino J, Barone V (2013) General Time Dependent Approach to Vibronic Spectroscopy Including Franck–Condon, Herzberg–Teller, and Duschinsky Effects. J Chem Theory Comput 9:4097–4115. doi: 10.1021/ct400450k
51. Muniz-Miranda F, Pedone A, Battistelli G, et al (2015) Benchmarking TD-DFT against Vibrationally Resolved Absorption Spectra at Room Temperature: 7-Aminocoumarins as Test Cases. J Chem Theory Comput 11:5371–5384. doi: 10.1021/acs.jctc.5b00750
52. Puzzarini C, Biczysko M, Barone V (2010) Accurate Harmonic/Anharmonic Vibrational Frequencies for Open-Shell Systems: Performances of the B3LYP/N07D Model for Semirigid Free Radicals Benchmarked by CCSD(T) Computations. J Chem Theory Comput 6:828–838. doi: 10.1021/ct900594h
53. Barone V, Biczysko M, Bloino J, Puzzarini C (2013) Glycine conformers: a never-ending story? Phys Chem Chem Phys 15:1358–1363. doi: 10.1039/C2CP43884D
54. Bloino J, Biczysko M, Santoro F, Barone V (2010) General Approach to Compute Vibrationally Resolved One-Photon Electronic Spectra. J Chem Theory Comput 6:1256–1274.
55. Barone V, Bloino J, Guido CA, Lipparini F (2010) A fully automated implementation of VPT2 Infrared intensities. Chem Phys Lett 496:157–161. doi: http://dx.doi.org/10.1016/j.cplett.2010.07.012
56. Biczysko M, Panek P, Scalmani G, et al (2010) Harmonic and Anharmonic Vibrational Frequency Calculations with the Double-Hybrid B2PLYP Method: Analytic Second Derivatives and Benchmark Studies. J Chem Theory Comput 6:2115–2125. doi: 10.1021/ct100212p
57. Banerjee S, Baiardi A, Bloino J, Barone V (2016) Vibronic Effects on Rates of Excitation Energy Transfer and Their Temperature Dependence. J Chem Theory Comput 12:2357–2365. doi: 10.1021/acs.jctc.6b00157
58. Hodecker M, Biczysko M, Dreuw A, Barone V (2016) Simulation of Vacuum UV Absorption and Electronic Circular Dichroism Spectra of Methyl Oxirane: The Role of Vibrational Effects. J Chem Theory Comput 12:2820–2833. doi: 10.1021/acs.jctc.6b00121
59. Frisch MJ, Trucks GW, Schlegel HB, et al Gaussian~09 {R}evision {D}.01.
60. Becke AD (1993) Density-functional thermochemistry. III. The role of exact exchange. J. Chem. Phys. 98:
61. Perdew JP (1986) Density-functional approximation for the correlation energy of the inhomogeneous electron gas. Phys Rev B 33:8822–8824.
62. Perdew JP, Burke K, Wang Y (1996) Generalized gradient approximation for the exchange-correlation hole of a many-electron system. Phys Rev B 54:16533–16539. doi: 10.1103/PhysRevB.54.16533
63. Dunning Jr. TH, Hay PJ (1977) Gaussian Basis Sets for Molecular Calculations. In: Schaefer III H (ed) Methods Electron. Struct. Theory SE - 1. Springer US, pp 1–27
64. Hay PJ, Wadt WR (1985) Ab initio effective core potentials for molecular calculations. Potentials for K to Au including the outermost core orbitals. J. Chem. Phys. 82:
65. Hay PJ, Wadt WR (1985) Ab initio effective core potentials for molecular calculations. Potentials for the transition metal atoms Sc to Hg. J. Chem. Phys. 82:
66. Wadt WR, Hay PJ (1985) Ab initio effective core potentials for molecular calculations. Potentials for main group elements Na to Bi. J. Chem. Phys. 82:
67. Cossi M, Scalmani G, Rega N, Barone V (2002) New developments in the polarizable continuum model for quantum mechanical and classical calculations on molecules in solution. J Chem Phys 117:43. doi: 10.1063/1.1480445
68. Barone V, Cossi M, Tomasi J (1997) A new definition of cavities for the computation of solvation free energies by the polarizable continuum model. J. Chem. Phys. 107:
69. Grimme S, Antony J, Ehrlich S, Krieg H (2010) A consistent and accurate ab initio parametrization of density functional dispersion correction (DFT-D) for the

94 elements H-Pu. J Chem Phys. doi: http://dx.doi.org/10.1063/1.3382344
70. Barone V, Bloino J, Biczysko M, Santoro F (2009) Fully Integrated Approach to Compute Vibrationally Resolved Optical Spectra: From Small Molecules to Macrosystems. J Chem Theory Comput 5:540–554. doi: 10.1021/ct8004744
71. Dennington, R.; Keith, T.; Millam J (2009) GaussView, Version 5.
72. Gorelsky SI (2009) AOMix: Program for Molecular Orbital Analysis. http://www. sg-chem.net
73. Gorelsky SI (2009) Swizard. http://www.sg-chem.net